



Signal Integrity on RDL and optimization of DAC digital values for Ge pixel detector testing

Askar Marzhan, Kazakh National University named after al-Farabi,
Almaty, Kazakhstan

September, 2015

Supervisors: Heinz Graftsma, Milija Sarajlic, David Pennicard

Abstract

Here is presented my work during the DESY Summer Student Programme 2015 in the FS-DS group. DESY is working on the development of a large area detectors. Nowadays DESY has a module of large area detector which is called LAMBDA and is preparing for experiments at high photon energies.

Signal Integrity on RDL and Optimization of DAC digital values are made and presented in this report.

First, equivalent scheme of RDL was simulated in Multisim Software and checked for time delay. Secondly, the quality of individual bump bonds on Ge sensor was determined by sweeping DAC digital values.

Contents

1. Introduction.....	3
1.1. Hybrid pixel detectors for synchrotron applications	3
2. Short theory	3
2.1. High-Z sensors	3
2.2. Germanium sensor	3
2.3. Medipix3 readout chip	4
2.4. LAMBDA module	5
2.5. RDL	6
3. Experiments and results	7
3.1. Signal Integrity on RDL	7
3.2. Optimization of DAC digital values for Ge pixel detector testing	10
3.2.1. Readout software	10
3.2.2. Sweeping Ikum	11
3.2.3. Sweeping Threshold0	13
4. Conclusion	15
5. Acknowledgement	15
6. References.....	15

1. Introduction

1.1. Hybrid pixel detectors for synchrotron applications

Hybrid pixel detectors[1] are currently the cutting-edge technology for a range of X-ray scattering and imaging experiments at synchrotrons. Generally, hybrid pixel detectors for X-ray detection such as Pilatus and Medipix2 work by comparing the signal pulses in each pixel to a threshold level, and counting the number of hits over threshold. As a result, these detectors can achieve excellent signal-to-noise performance, even when the X-ray flux arriving at a pixel is low, and can discriminate against lower-energy background photons. These detectors can also achieve high frame rates, making it possible to exploit the extremely high brilliance of modern X-ray beamlines (for example when performing time-resolved measurements, or scanning a sample with a focused beam).

Most hybrid pixel detectors use a silicon sensor. However, silicon sensors have low quantum efficiency at high photon energies, as shown in Fig. 1, which limits their use in experiments with hard X-rays.

Synchrotron beamlines designed for materials science frequently operate at higher energies. For example, the Petra-III synchrotron light source at DESY has one beamline which can operate at 150keV, and three beamlines which can produce beams of 50keV and above. These X-ray beams can be focused down to a small volume within a sample, making it possible to determine the material structure at a buried interface (in a fuel cell, for example) or to systematically map the interior structure of a sample (for example, to find the grain structure of a polycrystalline material). Using detectors with higher quantum efficiency will increase the speed and accuracy of these experiments, particularly when working with samples that are sensitive to radiation.

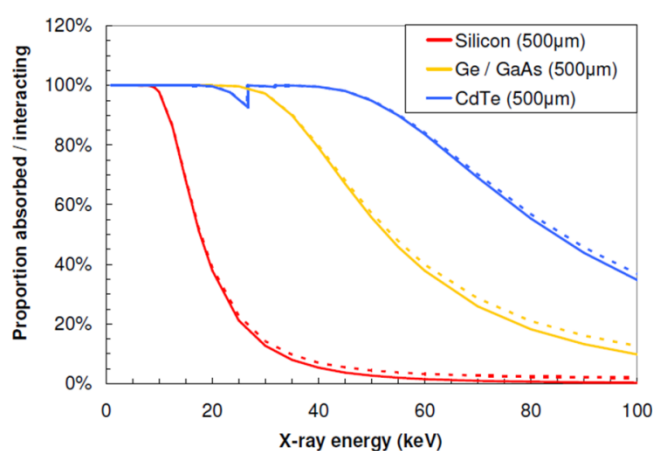


Figure 1. Photon absorption efficiency of different semiconductors.

2. Short theory

2.1. High-Z sensors

It is possible to use sensors made from “high-Z” (high atomic number) [2] semiconductors to achieve high quantum efficiency with hard X-rays.

Different high-Z materials have different strengths and weaknesses. One common problem is that most high-Z materials are compound semiconductors, which means that they typically have much higher defect densities than elemental semiconductors such as silicon. Fig. 1 depicts the absorption efficiencies of several semiconductor materials such as Si, Ge, GaAs and CdTe.

2.2. Germanium sensor

Germanium is an elemental semiconductor, which is available in reasonably large 6” wafers of high uniformity, with a doping concentration as low as 10^{10}cm^{-3} and negligible charge trapping. As a result, Ge is widely used for spectroscopic X-ray detectors. However, there are various barriers to using Ge in pixel detectors. DESY have worked with Canberra (Lingolsheim) and Fraunhofer IZM (Berlin) to produce germanium pixel detectors and bump-bond them to Medipix3 chips. The first disadvantage of germanium is its narrow bandgap of 0.67eV. This means that it has high leakage current, and cannot be operated at

room temperature. Typically, germanium photodiodes for spectroscopy are operated at liquid nitrogen temperature, in order to obtain a very low leakage current and hence achieve high energy resolution. However, photon-counting hybrid pixel detectors are more tolerant of leakage current, for two reasons. Firstly, due to the small volume of each pixel, the leakage current per pixel will be comparatively low. Secondly, photon-counting readout chips such as Medipix3 count the number of signal pulses arriving in each pixel, rather than integrating the total signal seen over the acquisition period, so leakage current will have less effect on their performance. A pixellated germanium detector with pixels of $55\mu\text{m}$ should have a leakage current of around 1nA per pixel at -50°C , which is safely below the design limit of 25nA .

The need for cooling places additional demands on the engineering of the detector system, and will tend to make the system more expensive and bulky. However, in experiments on a synchrotron beamline, this can be tolerated. Secondly, the technology for fabricating germanium sensors must be modified in order to produce small pixels. This is done by Canberra. Canberra's fabrication method first used lithium diffusion to create an ohmic n-type contact on the back surface of high-resistivity n-type germanium. Hence, p-doped diode junctions were produced on the front surface using photolithography and ion implantation of boron. The detector was completed by depositing aluminium contacts on the back surface and the pixel contacts, and then passivating the detector.

Indium was used to bump-bond this sensors to readout chip. This is for two reasons. Firstly, when the detector is cooled during operation, there will be a mismatch between the thermal contraction of the germanium sensor and the silicon readout chip. For a Medipix3-sized chip and a germanium sensor, and a temperature change of 100K , the difference in contraction at the edge of the sensor assembly will be $3.5\mu\text{m}$. This means the bump bond must be composed of a metal which remains ductile at low temperature, so that the bond flows to accommodate this small shift in position rather than cracking. Secondly, germanium is extremely temperature sensitive; heating it to above 100°C for extended periods can allow diffusion of impurities into the germanium, and may also damage the passivation. Due to indium's softness, it is possible to electroplate In bumps on both the sensor and readout chip, and then bond them together at less than 100°C using thermocompression. The bump-bonding of these sensors was done by Fraunhofer IZM (Berlin).

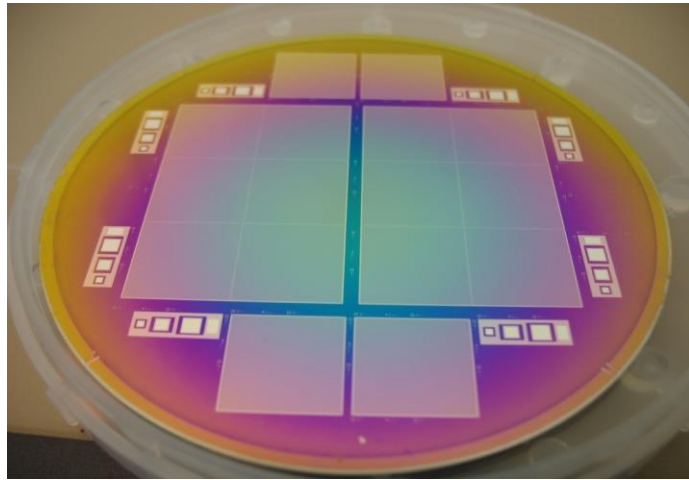


Figure 2. Ge sensors produced by Canberra France

2.3. Medipix3 readout chip

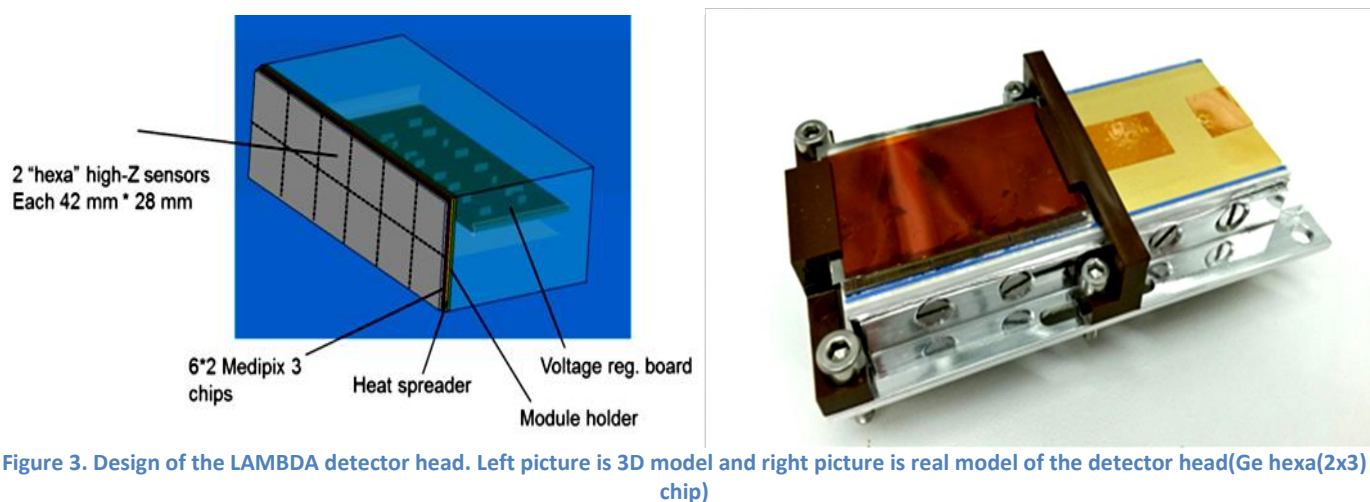
Medipix3[3] is a new generation of photon-counting readout chip, developed at CERN. It has a $256\text{-by-}256$ array of pixels, with a reasonably small pixel size of $55\mu\text{m}$. Additionally, Medipix3 has a range of new features which make it attractive for experiments at synchrotrons. Firstly, each pixel contains two counters. Since one counter can be used to count photon hits while the other one is being read out, this means that the detector can acquire and read out images continuously with negligible dead time. If the Medipix3 chip is read out at its maximum rate, then a readout rate of 2000 frames per second can be achieved with a counter depth of 12 bits, and even higher rates can be achieved by reducing the

counter depth. Secondly, the Medipix3 detector has a “charge summing” feature. If a photon generates signals in multiple neighboring pixels, the charge-summing circuitry can sum these signals together to reconstruct a single hit. This can allow better energy discrimination and ensures that no loss or double-counting of photon hits will occur.

2.4. LAMBDA module

Most synchrotron experiments require a larger detector area than can be provided by a single Medipix3 chip, to apply this readout chip to synchrotron beamlines larger multi-chip modules should be built. The LAMBDA (Large Area Medipix-Based Detector Array) [4] module has been designed to meet these requirements.

The prototype LAMBDA[5] module consists of a detector head plus a digital board for readout. The basic design of the detector head is shown in Fig. 3. It comprises a ceramic “module holder” circuit board, on which detector assemblies can be mounted, and a voltage regulator board, which powers the detector assembly and also carries the signal lines between the detector and the readout system.



The Medipix3 chip can be connected to readout electronics by wire-bond pads along one side (Fig. 4), which means that an “N-by-2” chip module layout is possible. A 6-by-2-chip layout was chosen. This means that the module can be used with a single large silicon sensor or two “hexa” size high-Z sensors of 42 mm by 28 mm. This is the biggest Medipix3-compatible sensor size that can be obtained from a 3” wafer, which is a typical size for high-Z materials. The 12-chip module will generate approximately 18 W of heat during operation, and some high-Z materials such as germanium require cooling during operation. As shown in Fig. 4, the module ceramic is mounted on a cooling block, which can then be cooled to low temperature. The voltage regulator board is connected to the back surface of module ceramic with a high density connector. The voltage regulator board and the rest of the readout system sit immediately behind the sensor, thus making it possible to tile multiple modules together to cover a large area (albeit with some dead areas between modules). Then the voltage regulator board is connected to a readout board. For the current system, a prototype readout board has been developed which uses an FPGA to control and read out the chip, and an USB2 interface to communicate with the control PC. The Lambda module is read out at a high frame rate, using a readout board with 10 Gigabit Ethernet links.

2.5. RDL

TSV-through silicon via technology (Fig. 4, bottom picture) is a vertical electrical connection passing completely through a silicon wafer or die. This technology gives an alternative connection between the Medipix3 chip Input-Outputs (IO) and readout system which significantly improves the percentage of active area. This technology will be used in the future. Our module based on wire bonded technology (Fig. 4, above picture).

RDL is a redistribution layer. Fig. 5 shows logic schematic of the RDL. There are three primary uses for RDL here. The first is to move the bond pads around the face of the die for flip-chip applications. It is important to spread the contact points around the die so that solder balls can be applied and the stress of mounting can be spread. Another important application of RDL involves die stacking. In this application, similar die can be mounted in a single package. In order to give each die a unique address, the address lines of each die can be placed in a unique location. A third application for RDL is simply to move the bond pads of a device to a position more convenient or accessible for subsequent bonding and packaging steps. This may include matching the layout of an old die that is no longer being supported and must be replaced by a newer design.

RDL is a process that generally involves one or two layers of metal and two or three layers of a polymer dielectric material (Fig. 6).

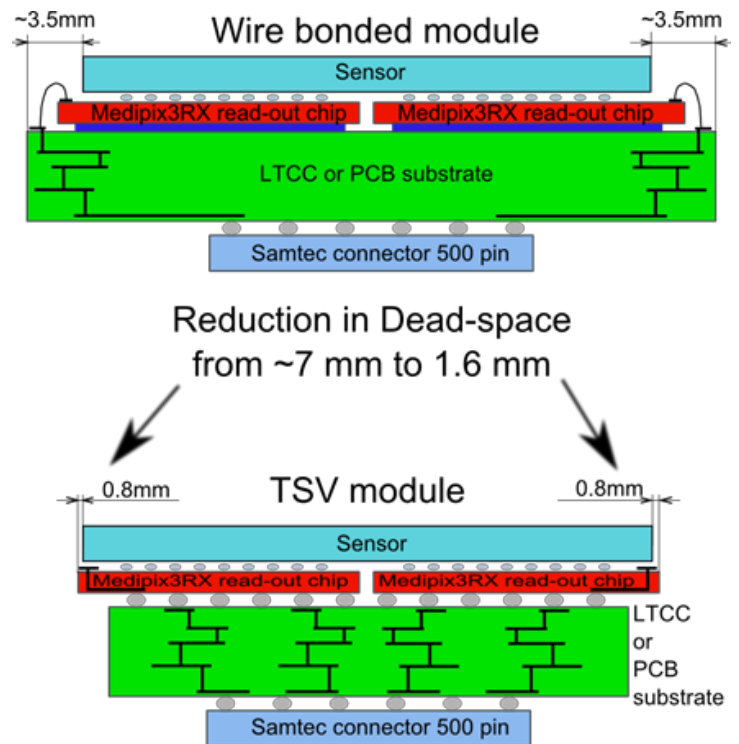
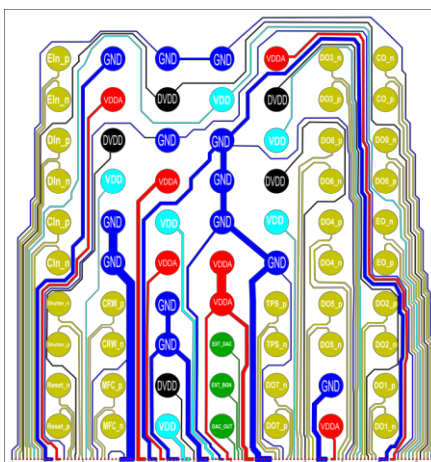


Figure 4. Cross-section diagram of the module holder with a sensor assembly mounted on it.



VDDA VDD
GND DVDD

Figure 5. Logic model of RDL

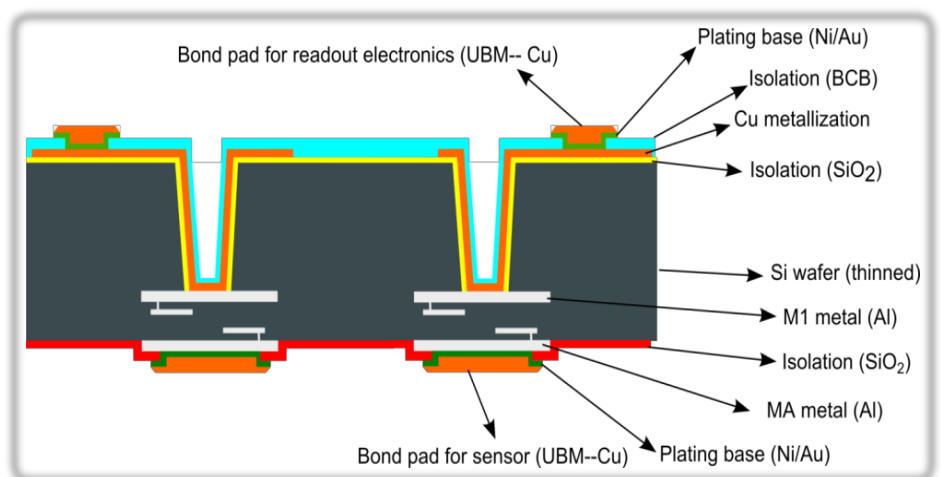


Figure 6. Cross-section diagram of the RDL

3. Experiments and results

3.1. Signal Integrity on RDL

Before taking images and dates from chip, we need determine the signal Integrity and time delay on RDL.

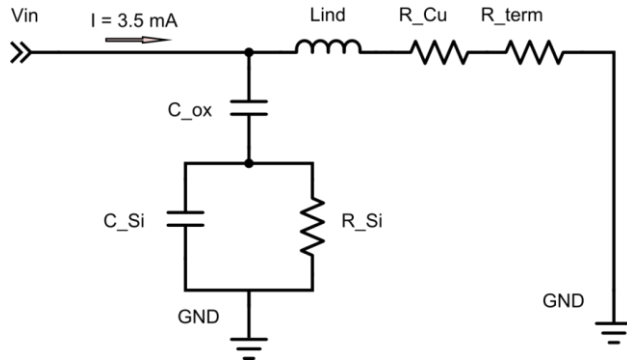


Figure 7. Equivalent scheme of RDL

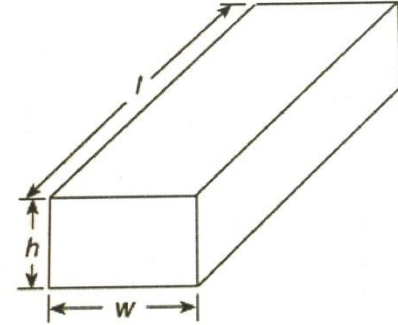


Figure 8. Straight rectangular copper

Equivalent scheme of RDL is shown in Fig. 7. Lind is considered as a straight rectangular copper trace pair. Here radiocomponents C_{Si}, C_{ox}, R_{Si}, R_{Cu} and Lind are capacitance of silicon, capacitance of oxide, resistance of silicon, resistance of copper trace and inductance of copper pairs. To implement this scheme, it is necessary to know their values.

Using the formulas shown below[6], we calculated each values:

Inductance of each copper trace:

$$L = 2l * 10^{-7} \left[\log \left(\frac{2l}{R} \right) - 1 + \frac{R}{l} \right] = 2,1004 * 10^{-8} H,$$

where $l = 15mm$ is a length of trace, $R = 0,2235(h + w)$, $w = 40\mu m$, width and $h = 5\mu m$ height of trace.

Mutual inductance between copper pairs:

$$M = 2l * 10^{-7} \left[\log \left(\frac{2l}{d} \right) - 1 + \frac{d}{l} \right] = 1,4797 * 10^{-8} H,$$

where d is distance of copper pairs comparing their center ($d=2w$).

Common inductance is

$$Lind = 2(L - M) = 1,2414 * 10^{-8} H.$$

Capacitances of oxide and silicon:

$$C_{ox} = \frac{\epsilon \epsilon_0 S}{d} = 20,709 pF; \quad C_{Si} = 0,31 pF,$$

where $\epsilon = 3.9$ for oxide and $\epsilon = 11.68$ for silicon, $d_{ox} = 1\mu m$, $d_{Si} = 200\mu m$, $S = l * w$.

Resistance of copper and silicon:

$$R_{Cu} = \frac{\rho l}{S} = 1,260 \Omega m; \quad R_{Si} = 2500 \Omega m,$$

where $\rho = 10 \Omega m * cm$ for Si, $\rho = 1.68 * 10^{-6} \Omega m * cm$.

Thus we simulated our scheme in software Multisim. Multisim is a wide spread software and comfortable to use with its many tools. In our scheme we used radiocomponents and measurement devices as shown in Fig. 9. Here U1, U2, U3 are amperemeters, XFG1 is functional generator, XSC1 is oscilloscope, XBP1 is bode plotter, XNA1 is network analyzer.

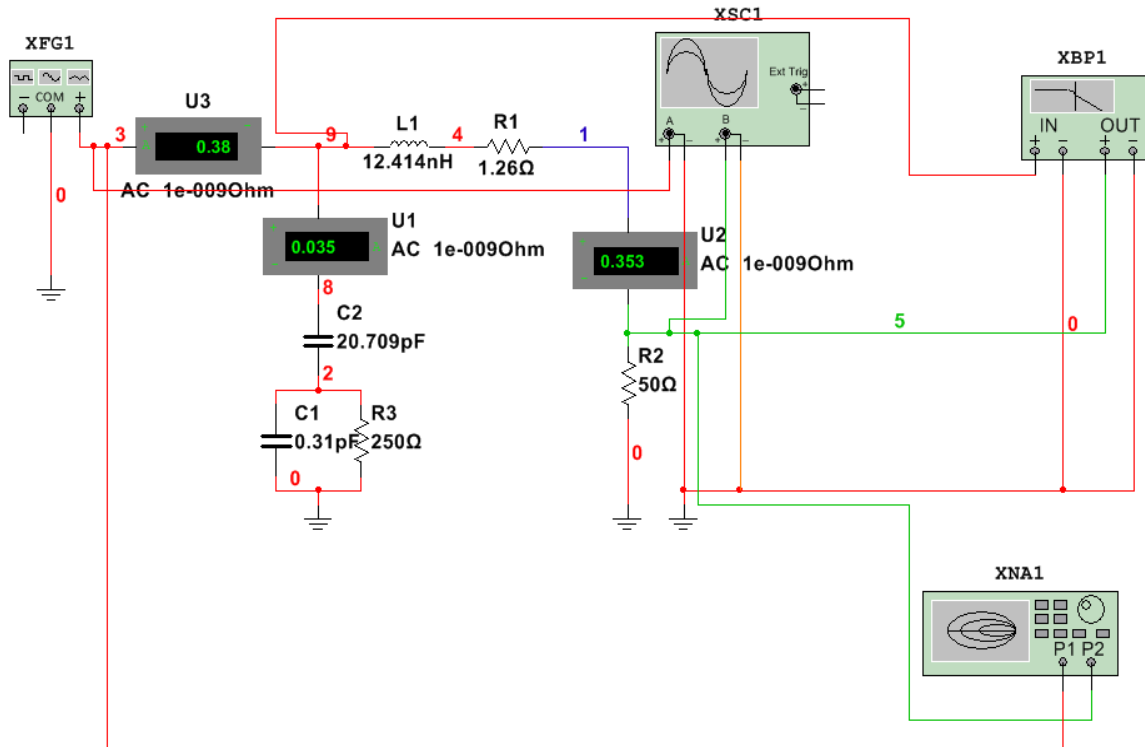


Figure 9. Simulation of equivalent scheme of RDL in Multisim software.

With help of oscilloscope, we were able to see the time diagram of input and output signals on RDL (Fig. 10).

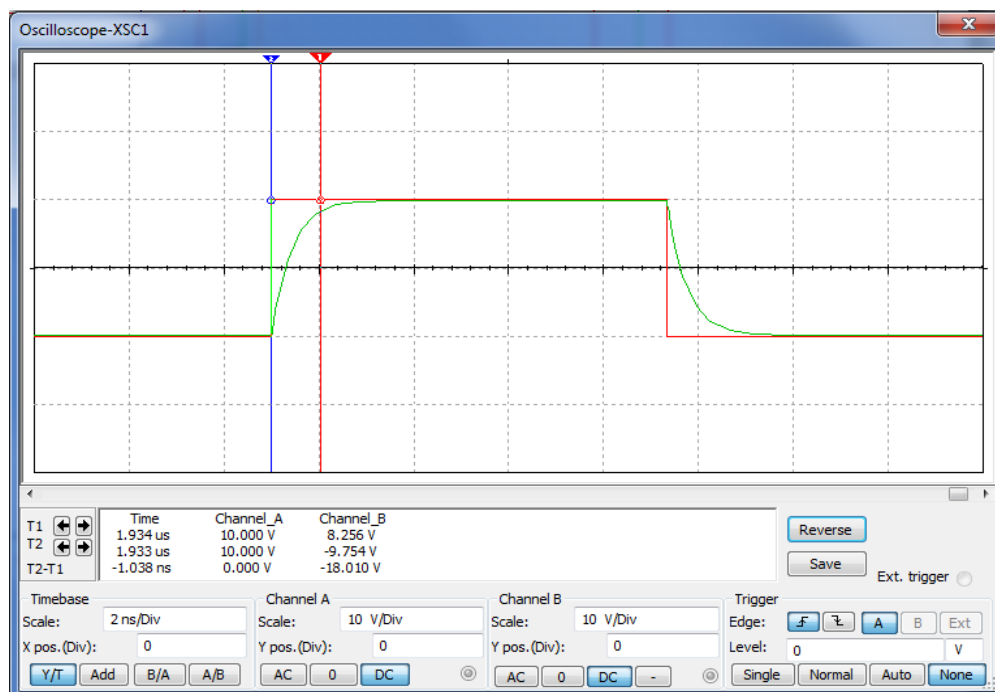


Figure 10. The time diagram of input and output signals on RDL

As shown above, the input signal is given as a rectangular signal from functional generator (red line), and output signal (green line) has some time delay. It takes approximately 1ns to approach from the positive edge of rectangular signal to 90% of maximal value, this is the time delay. 1ns is a small value but not negligible.

In Multisim software using bode plotter, it is possible to determine the dependence of Insertion loss of the signal on the frequency.

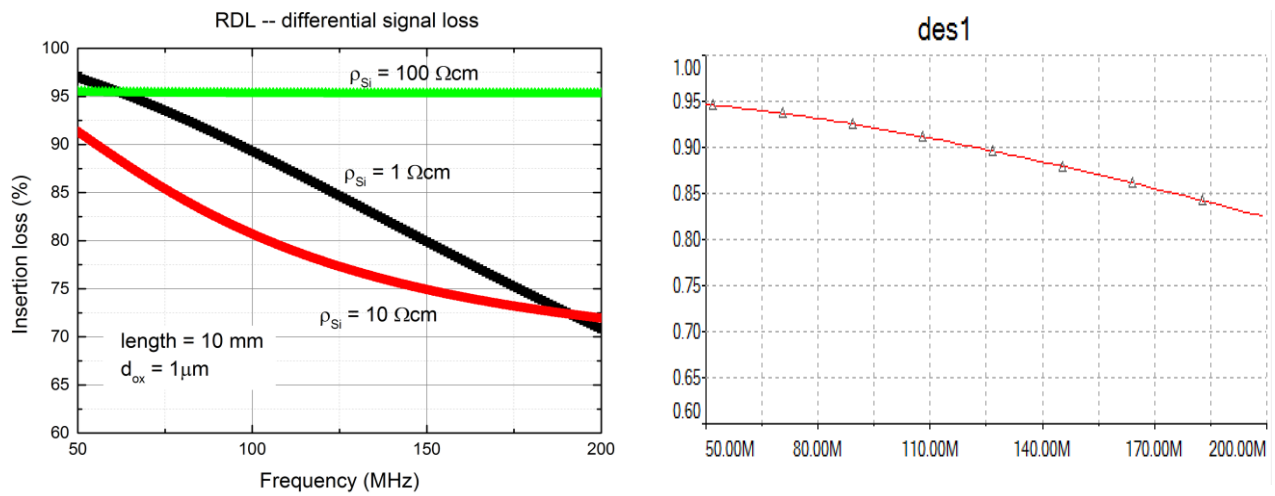


Figure 11. Dependence of Insertion loss on frequency (left picture is analytic calculation and right picture is numerical calculation)

We did numerical calculation and compared with analytic version, in Fig. 11 (we should compare it with black line, because the parameter of our scheme is suitable with its parameter, $\rho_{Si} = 1 \text{ Ohm} * \text{cm}$). From the picture we can see that numerical calculation is better than analytic calculation, because in analytic variant it is going down from 97% until 70%, but in numerical it is only until 83%. This explains the operation of RDL at high frequencies.

3.2. Optimization of DAC digital values for Ge pixel detector testing

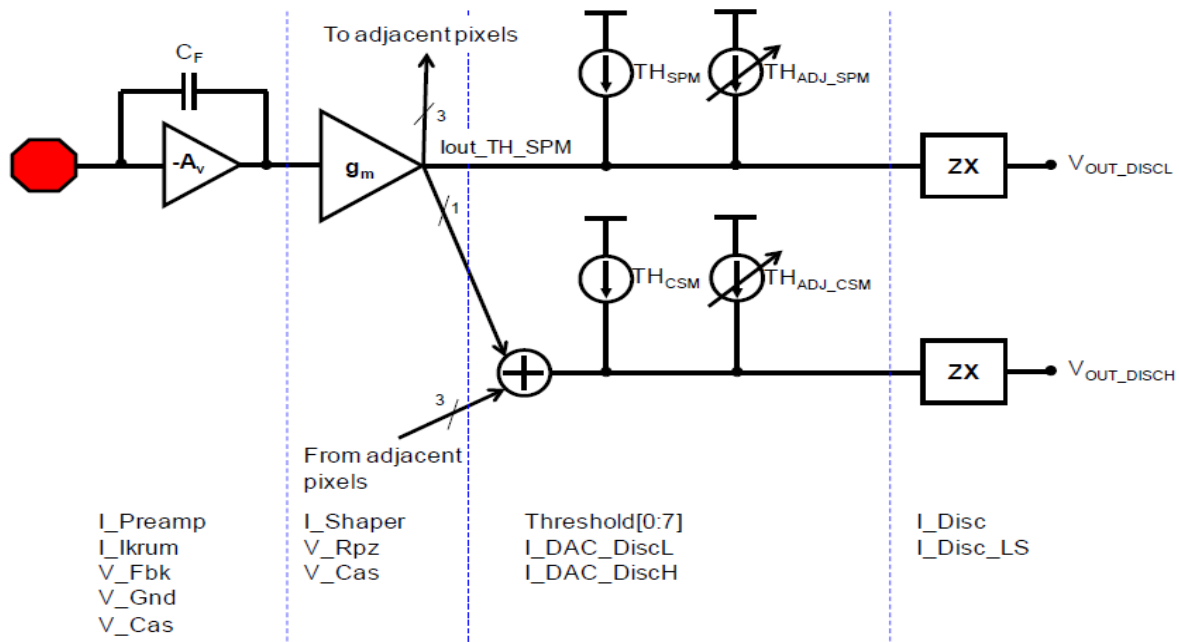


Figure 12. Scheme of the detector module for one pixel

The above picture, schematic of the module, depicts that each DAC digital value control different part of the device. DAC is Digital-to-Analog Converter that produce reference voltage or current in Medipix3 chip. To optimize the work of the detector and improve its quality Optimization of DAC digital values is very important.

3.2.1. Readout software

Before Optimization we need to talk about readout software. It is called "HEXA test" and written in C++. In Fig. 13 is shown its window. There are four tabs here: MATRIX, DAC SETTINGS, TEST and Ge_TEST. But two of these are important for our experiments: DAC SETTINGS and Ge_TEST. On the tab DAC SETTINGS we can set all of DAC digital values independently, it makes easily to find optimal DAC values to get good images.

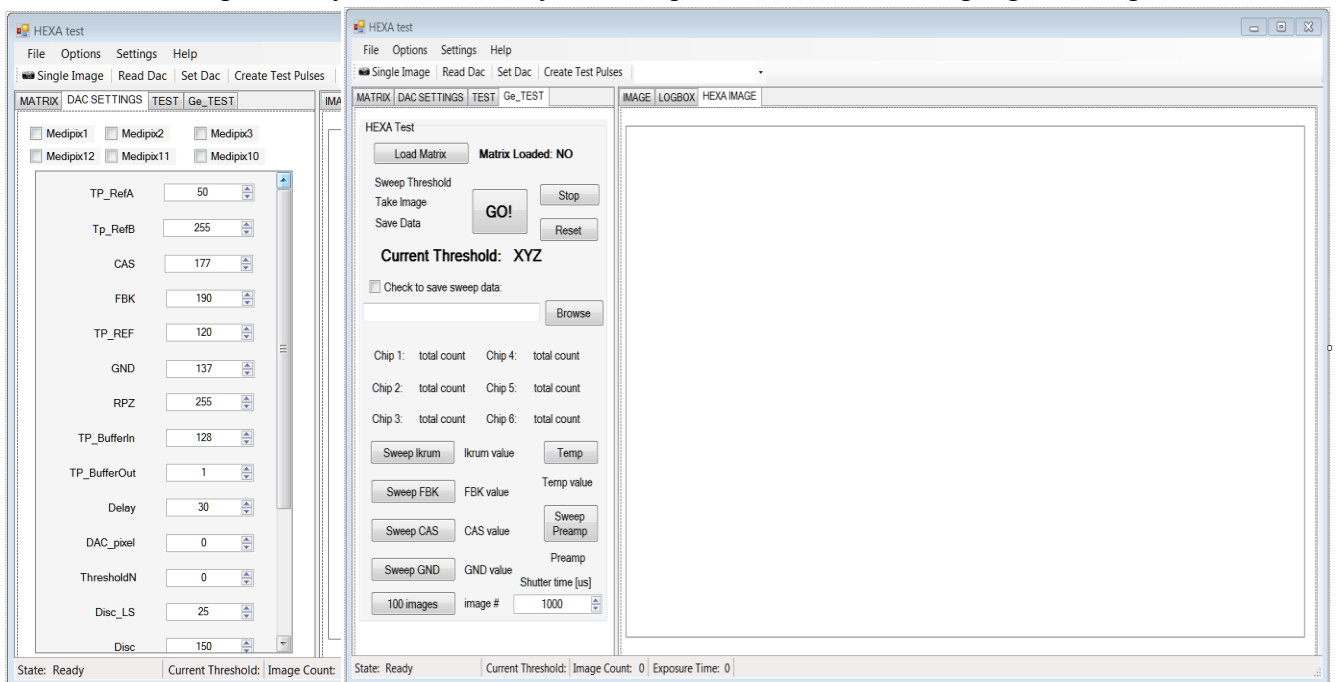


Figure 13. The window of software intended to test Ge hexa sensor

And on the next tab, Ge_TEST, we can sweep DAC digital values, by changing from 0 to 255 one by one. Here it is possible to sweep DAC values such as Threshold0, Ikrum, FBK, CAS, GND, Temp and Preamp. The data coming from sensor will be shown as an image on the big white window which is called HEXA IMAGE. Sweeping Threshold0 is realized clicking the button "GO!", if we need to save the images, we should click "Check to save sweep data" and "Browse".

Before acquiring data we loaded zero values in counter 1 by clicking the button "Load Matrix", this moved all thresholds to maximum value.

The main goal of this experiment is to determine the number of the pixels that are bump bonded correctly from the Ge sensor to the Medipix readout chip. For this purpose we did some operations [7]: sweeping DAC values collected images and made them analyzes using Matlab software. We swept Ikrum and Threshold0, other DAC values was fixed (Tab. 1).

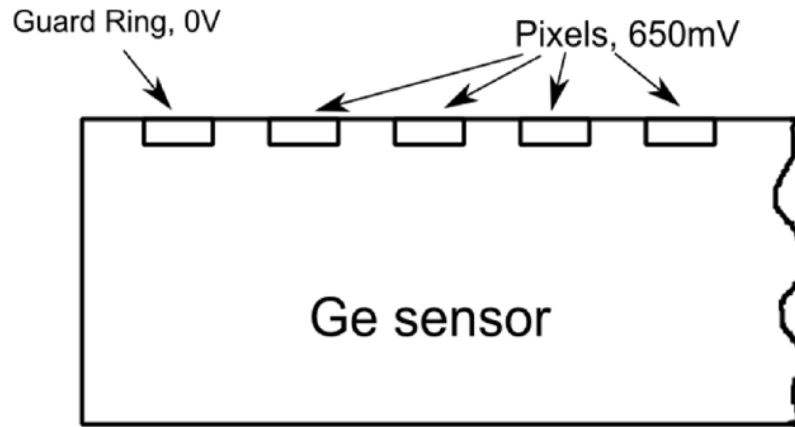


Figure 14. Schematic representation of the Ge sensor corner.

Fig. 14 shows the structure of the sensor corner, here the guard ring and some pixels are visible. Even the polarization voltage equal to zero ($HV=0V$), there will be potential difference between pixels and the guard ring. This will cause leakage current to flow from

Tab. 1 DAC values for different measurements						
	<i>Ikrum</i>	<i>FBK</i>	<i>CAS</i>	<i>GND</i>	<i>Preamp</i>	<i>Th1</i>
1	5	130	170	100	100	20
2	250	130	170	100	100	20

guard ring to the direction of the sensor's center.

To minimize the leakage current in the edge pixels, the detector must be tested in lower temperatures. For this we used the climate chamber and cooled the detector on the temperature $-40^{\circ}C$. Cooling the working atmosphere the leakage current will be minimized and edge pixels will be able to count hits.

As it is told above, Threshold0 is moved to the highest value, this is needed in order to have most of the pixels counting on different threshold values. If the hits are under the threshold value, they will be ignored by the device.

3.2.2. Sweeping Ikrum

The preamplifier circuit schematic is shown in Figure 5.12. In red, the Charge Sensitive Amplifier[8] is shown. The amplitude of the output voltage pulse (V_{out}) is proportional to the induced charge in the input node (V_{in}). The preamplifier implements a leakage current compensation network (shown in green in Fig. 15). A positive leakage current (DC current from the detector entering the preamplifier) can be sunk by M_{LEAK} . The implemented

circuitry can also deal with a negative leakage. The maximum leakage current that the detector can sink from the preamplifier circuit is $I_{Krum}/2$.

I_{Krum} current is used to discharge the capacitor (Fig.15) and compensate the leakage current. That is why the sweeping I_{Krum} is more important than other DAC values. I_{Krum} value was swept from 0 to 256 one by one, and for each I_{Krum} value was taken noise image.

Fig. 16 shows the evolution of the hexa noise images during I_{Krum} sweep and there are shown the I_{Krum} values for every image.

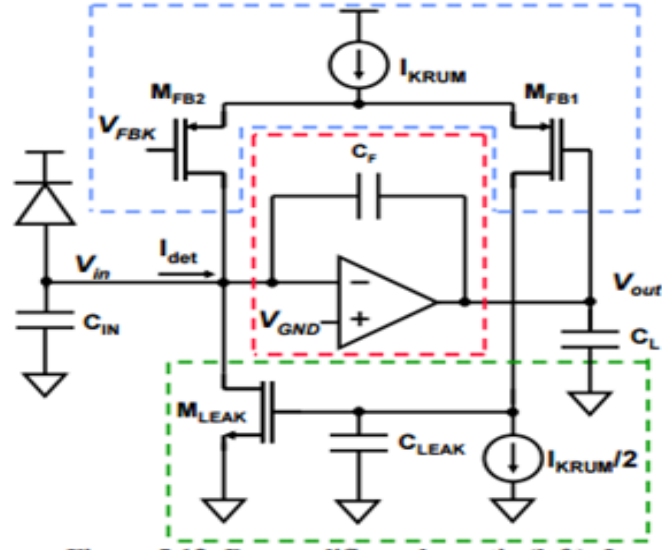
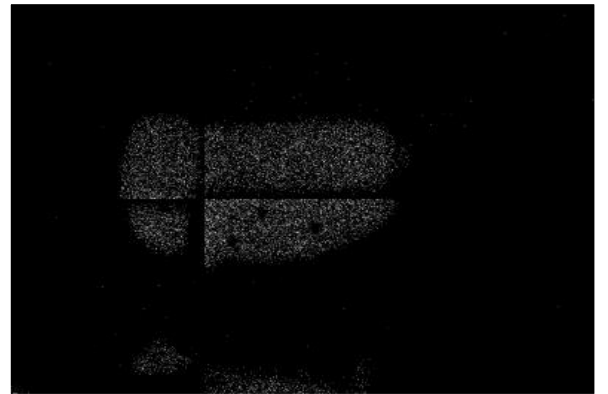


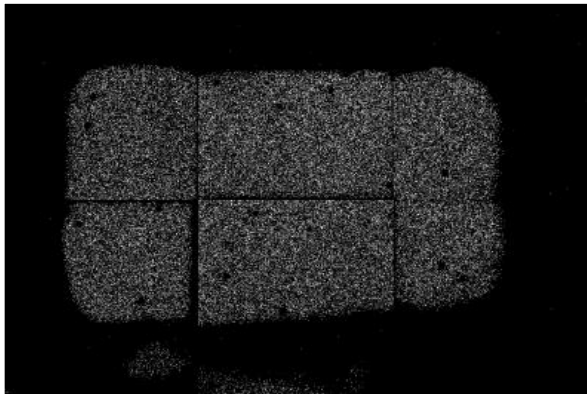
Figure 15. Preamplifier schematic. The feedback reset path and the leakage compensation feedback are shown in blue and green respectively.



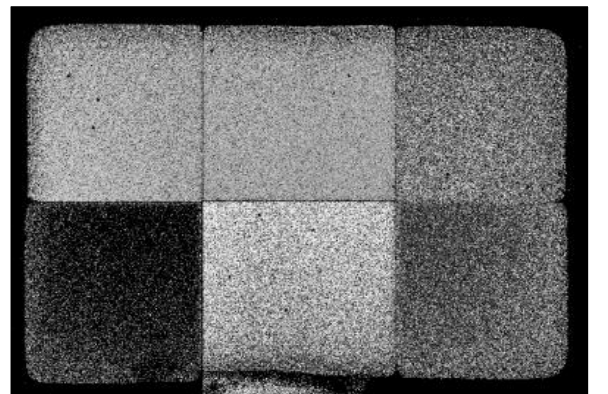
a)



b)



c)



d)

Figure 16. Evolution of the hexa noise image during I_{Krum} sweep. I_{Krum} values a)=10, b)=23, c)=45, d)=252.

Collecting all images, we did dependence diagram as shown in Fig. 17.

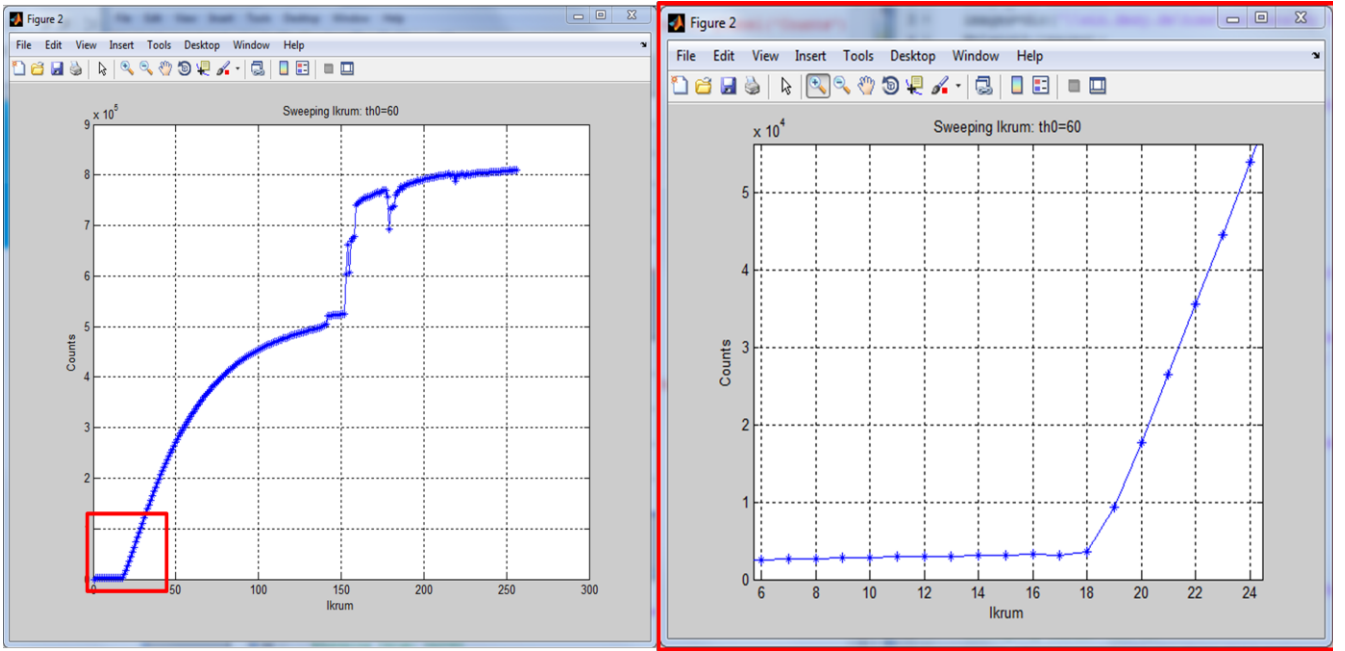


Figure 17. Dependence of the amount of counts on Ikum value

Left diagram depicts that at low Ikum values there are no counts, increasing it until 256, amount of counts grows faster. But zooming the beginning area of diagram (right picture), we can see some counts. While Ikum value is low, all pixels are flooded by leakage current, it renders them non-responsive. That is why we assume that these counts are coming from the noise within Medipix itself and these pixels are believed to be not bonded correctly. But with high Ikum value small part of the pixels are still non-responsive.

3.2.3. Sweeping Threshold0

In order to collect all pixels which are responsive on different Ikum values we set Ikum to specific value and sweep Theshold0 from zero to 200 digital values. Pixels which are noisy on threshold sweep with Ikum value 5 are not bump bonded and are presented in Fig. 20 in red color. Pixels which are noisy on Ikum value 250 are bump bonded correctly and presented in Fig. 20 in white. Pixels which are always silent are presented in Fig. 20 in black and they are considered to be bumped correctly because we assume that non-responsiveness is the consequence of the excessive Leakage Current in these pixels and this influence cannot be reduced by modifying Ikum value.

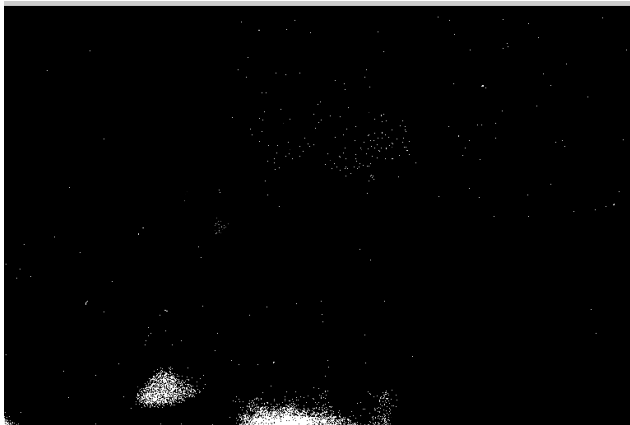


Figure 18. Non-bonded pixels (white spots)



Figure 19. Non-responsive pixels (black spots)

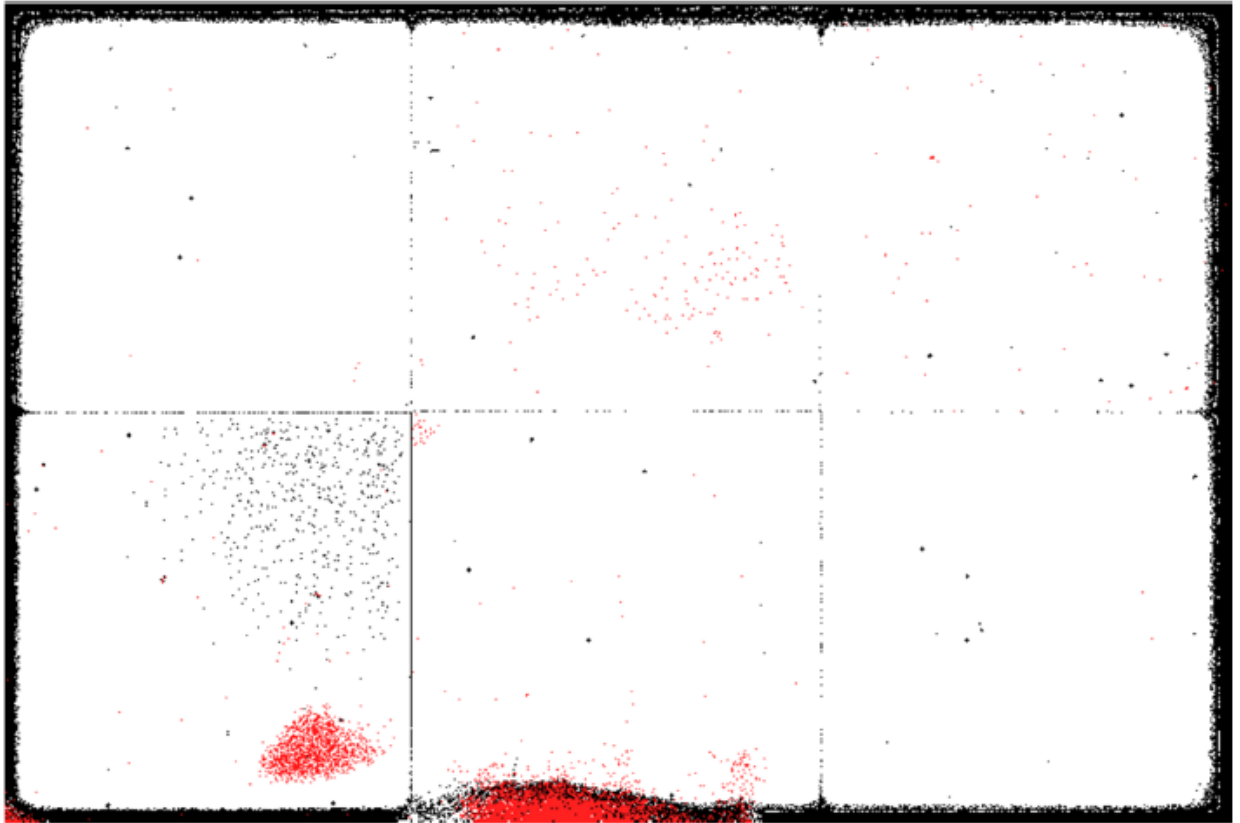


Figure 20. Final results of the measurements (compound image). Non-bonded pixels are red, non-responsive pixels are black and white area depicts responsive pixels

Also collecting all 200 images, we did diagram (Fig. 21). From the diagram we can see that at the Threshold0 values between 50-80, we can get all responsive pixels.

In total, there are 3739 non-bonded pixels which is 0.95% of all pixels.

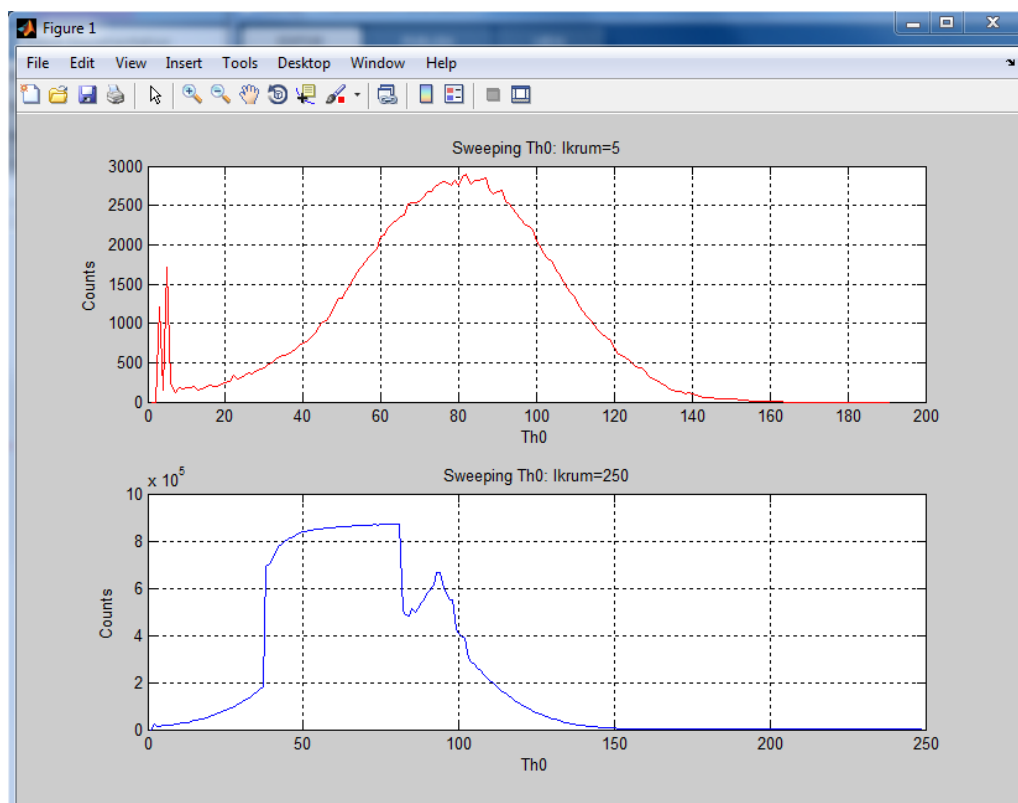


Figure 21. Sweeping Threshold0 value

4. Conclusion

Doing these experiments, we showed it is possible to estimate quality of bump bonds on Ge module. Also we determined that more than 99% of pixels are correctly bump bonded. We estimated Signal Integrity of RDL for TSV module by using Multisim software. Signal Integrity results are comparable with analytical modeling.

5. Acknowledgment:

First of all I am grateful to leader of FS-DS Heinz Graafsma for giving me opportunity to work with their group. Then I would thank to my supervisors Milija Sarajlic and David Pennicard for their help, their kindness, their patient, they taught me for many things during this Summer Programme and helped me. Also I want to express my gratitude to all members of the group for their friendly atmosphere, their goodness and support, and to DESY organizers. At the end I acknowledge to my teacher at my university Ahmet Saiymbetov for informing me about this program.

6. References:

- [1]C. Ponchut, J.L. Visschers, A. Fornaini, H. Graafsma, M. Maiorino, G. Mettivier and D.Calvet, *Evaluation of a photon-counting hybrid pixel detector array with a synchrotron X-ray source*. Nuclear Instruments and Methods in Physics Research A 484 (2002) 396–406
- [2]David Pennicard, Sabine Sengelmann, Sergej Smoljanin, Helmut Hirsemann, Heinz Graafsma, *Development of high-Z sensors for pixel array Detectors*
- [3]Milija Sarajlic, *Medipix calibration experiments and theory*. Medipix sensor testing at DESY from 01. 09. to 30. 11. 2010
- [4]Photon-science public web page: http://photon-science.desy.de/research/technical_groups/detectors/projects/lambda/index_eng.html
- [5] David Pennicard, Sabine Lange, Sergej Smoljanin, Julian Becker, Helmut Hirsemann, Michael Eppleb and Heinz Graafsma, *Development of LAMBDA: Large Area Medipix-Based Detector Array*, 2011 IOP Publishing Ltd and SISSA
- [6]Edward B. Rosa, *Bulletin of the Bureau of Standards: The self and mutual inductances of linear conductors*. [Vol. 4, No. 2]
- [7]Milija Sarajlic, *Germanium hexa sensor*. Report on measurements 20. 08. 2015 at DESY
- [8]Rafael Ballabriga Suñé, *The Design and Implementation in 0.13 μ m CMOS of an Algorithm Permitting Spectroscopic Imaging with High Spatial Resolution for Hybrid Pixel Detectors*, Tesi Doctoral.